Synthesis and characterization of organic bentonite using Gujarat and Rajasthan clays

Hasmukh A. Patel, Rajesh S. Somani, Hari C. Bajaj and Raksh V. Jasra*

Silicates and Catalysis Discipline, Central Salt and Marine Chemicals Research Institute, G.B. Marg, Bhavnagar 364 002, India

Indian bentonite collected from two different sources, namely Barmer district, Rajasthan and Cutch district, Gujarat was screened and purified using the well-known Stoke's law of sedimentation by dispersing different concentrations of bentonite (0.5, 1, 2, 3 and 4%) in deionized water. Chemical composition and cation exchange capacity of raw and purified bentonite (sedimented at different amounts of bentonite) were determined. Quantification of montmorillonite content was carried out using the cylinder enrichment method. Bentonite purified at lower concentration shows improvement in brightness index. Raw and purified bentonite samples were also studied by FT-IR and powder X-ray diffraction. Organic bentonite was prepared by treating the purified bentonite with quaternary ammonium salts (cetyltrimethylammonium bromide and strearyldimethylbenzylammonium chloride) and characterized by FT-IR, powder X-ray diffraction, CHN, TGA analysis and particle size distribution.

Keywords: Beneficiation, bentonites, montmorillonite, organoclays, sedimentation.

BENTONITE is smectite group clay formed from the alteration of siliceous, glass-rich volcanic rocks such as tuffs and ash deposits. The major mineral in bentonite is montmorillonite, having hydrated sodium, calcium, magnesium and aluminum silicate. Sodium and calcium are interchangeable ions giving montmorillonite a high ion exchange capacity[1,2]. Bentonite is used in a wide range of applications such as drilling mud, foundry sand binding, iron-ore pelletizing and civil engineering uses such as waterproofing and sealant[3]. Bentonite has excellent rheological and adsorption properties[4–6]. Sodium bentonite has a high swelling capacity and forms gel-like masses when added to water. Calcium bentonite has a lower swelling capacity than sodium bentonite. Normally the sodium-exchanged bentonite does not have as high a swelling capacity as natural sodium bentonite[7]. The significance of bentonite has increased due to its ability to form organically modified clays or nanoclays, which are gaining a large market place in the field of polymer nanocomposites, paints, greases, inks, cosmetics, wastewater treatment and drug-delivery vehicle in the last decade[8].

*For correspondence. (e-mail: rvjasra@csmcri.org)

The largest sodium bentonite deposits are located in Western United States in Wyoming, Montana and South Dakota. These sodium bentonites are also called Western or Wyoming bentonites, which indicates high-swelling sodium bentonite. Other smaller sodium bentonite deposits occur in Argentina, Canada, China, Greece, Georgia Republic, Morocco, South Africa, Spain and India[9–12]. Bentonite found in the Rajasthan and Gujarat in India is different from that available in the rest of world in terms of its chemical composition and higher iron content, which gives it a brownish-yellow colour. Purity of bentonite plays a crucial role in many applications, especially polymer nanocomposites, drug delivery vehicle and cosmetics. Organoclays or nanoclays synthesized from impure bentonite show haziness in polymer nanocomposite films and also limited exfoliation of layered silicates during processing of nanocomposites[8].

In the present communication, we have used Indian bentonites of Barmer district, Rajasthan and Cutch district, Gujarat to study their purification under different concentrations using Stoke's law of sedimentation. Raw and purified bentonite samples were characterized for their chemical composition, cation exchange capacity (CEC), swelling volume, FT-IR and powder X-ray diffraction techniques[13–15]. Sedimentation studies were carried out using the well known Stoke's equation as given below:

$$r^2 = \frac{9\eta h}{2(d1-d2)gt},$$

where r is the radius of the given particle (assuming spherical, in micron), h the height (cm) through which it falls in time t (s), g the acceleration due to gravity (9.8 m/s^2), $d1$, $d2$ the densities of solid and liquid respectively, and η the viscosity of water. Montmorillonite content was also calculated using the cylinder enrichment (CE) method[16]. Kaufhold *et al.*[16] have explained the quantification of montmorillonite in bentonite by different methods, and have concluded that the CE method is better than others because determination of layer charge is not required in cylinder enrichment, the influence of variable charge can be neglected and specific adsorption mechanism would not affect the quantification.

Bentonite lumps were collected from Barmer district (B) and the Cutch district (A). Quaternary ammonium salts, cetyltrimethylammonium bromide [$(CH_3)\cdot N\cdot(CH_2)_{15}CH_3\cdot Br$] and strearyldimethylbenzylammonium chloride [$(CH_2)_{17}CH_3\cdot(CH_3)_2\cdot N\cdot C_6H_5CH_2\cdot Cl$] were purchased from Aldrich and used as received. Chemical composition of raw clay (A and B) and purified bentonite (B0.5, B1, B2, B3, B4 and A0.5, A1, A2, A3, A4) was estimated by gravimetric analysis (wet chemical analysis which includes precipitation of silica, alumina, iron oxide and titania), CEC by standard ammonium acetate method, swelling volume by adding 2 g of bentonite in 100 ml deionized

water, allowing to stand for 24 h and noting the swelling volume. Brightness indices of raw and purified bentonite with reference to magnesium carbonate block were measured by PEI Digital reflectance meter. Powder X-ray diffraction (PXRD) analysis was carried out with a Phillips powder diffractometer X'Pert MPD using PW3123/00 curved Cu-filtered Cu-Kα (λ = 1.54056 Å) radiation with slow scan of 0.3°/s. Fourier transform infrared spectra (FT-IR) of raw and purified bentonites were measured with Perkin-Elmer Spectrum GX-Spectrophotometer as KBr pellet. Particle size analysis (under dry conditions) was done on Malvern Instrument–Master sizer 2000 at a feed rate of 50% and air pressure of 1 bar. Carbon, hydrogen and nitrogen (CHN) analysis of organically modified bentonite was carried out using a Perkin-Elmer CHNS/O analyser (Series II, 2400). Thermogravimetric analysis of organoclay and purified clay was carried out (Mettler–Toledo (TGA/SDTA 851e) thermal analyser) up to 850°C at the rate of 10°C/min and air flow of 40 ml/min.

Purified clay fractions were obtained by dispersing 50, 100, 200, 300 and 400 g of bentonite clay lumps (collected from Barmer district) in different buckets containing 10 l of deionized water (0.5, 1, 2, 3 and 4% clay slurry), and allowed to swell overnight, and then stirred for 30 min. According to the Stoke's law of sedimentation, the supernatant slurry having desired clay particle size (<2 μm) was collected after the pre-calculated time (10 h) and height (15 cm) at room temperature (30°C). The bentonite slurry was then dried at 90°C, ground, sieved through 200 mesh and designated as B0.5, B1, B2, B3 and B4 respectively. The same procedure was employed for bentonite lumps collected from Cutch district, which were designated as A0.5, A1, A2, A3 and A4. CEC of raw bentonite (A, B) and purified bentonite (B0.5, B1, B2, B3, B4 and A0.5, A1, A2, A3, A4) samples measured using standard ammonium acetate method at pH 7.0, montmorillonite content by CE method and swelling volume by standard method are shown in Table 1. In the CE method, 15 g of purified bentonite samples was dispersed in 1 l deionized water using ultrasonic dispersion. The suspension was transferred into 1 l glass cylinders (diameter ~5 cm) and kept in an oven at 60°C until the water is evaporated. From the top side of the sediment, 0.5 g of sample from each cylinder was removed using a sharp knife. These materials were equilibrated for 7 days at 50–60% relative humidity in order to regain the expansion capacity. Finally, the CEC was determined using standard ammonium acetate method and montmorillonite content (% w/w) with respect to its original CEC of purified samples was calculated.

One litre clay slurry of purified fraction B0.5 was heated at 80°C. Next 91 meq of organic modifiers, namely cetyltrimethylammonium bromide and strearyldimethylbenzyl ammonium chloride were dissolved in 500 ml distilled water and then added to the clay slurry at 11.11 ml/min using a peristaltic pump, with vigorous stirring at 80°C. The resulting organoclay slurry was filtered and washed with distilled water until it was free from halide ions. Organoclays were then dried overnight at 30°C, and subsequently at 110°C for 2 h, ground to pass through 200 sieve and designated as CTA-clay and SMB-clay respectively.

Chemical analysis, CEC and montmorillonite content of the different samples clearly demonstrate that sedimentation carried out at lower weight percentage of clay (B0.5, B1 and B2) yields bentonite free from non-clay impurities. As the concentration of clay increases, the viscosity of clay slurry increases which in turn makes sedimentation of the non-clay particles (greater than 2 μm) difficult. Montmorillonite content (87% w/w) and swelling volume (24 cc/ml) of samples purified by sedimentation at lower concentration (B0.5 and B1) is higher compared to raw and purified bentonites at higher concentration (B2, B3 and B4) as shown in Table 1. The brightness indices of purified bentonite obtained by sedimentation at lower concentration (B0.5, B1) is also

Table 1. Cation exchange capacity (CEC) and montmorillonite (MMT) content, swelling volume and brightness indices of raw (A and B) and purified (B0.5, B1, B2, B3, B4 and A0.5, A1, A2, A3, A4) bentonites samples

Sample	CEC (meq/100 g of clay)	CEC by CE method (meq/100 g of clay)	MMT content (% w/w)	Swelling volume (cc/ml)	Brightness index
B (raw)	64	–	–	16	54
B4 (4%)	67	88	76	16	55
B3 (3%)	72	93	77	17	55
B2 (2%)	80	97	82	21	57
B1 (1%)	91	104	87	24	60
B0.5 (0.5%)	91	104	87	24	60
A (raw)	61	–	–	21	53
A4 (4%)	62	83	74	21	53
A3 (3%)	77	91	84	21	53
A2 (2%)	81	95	85	25	56
A1 (1%)	88	102	86	29	58
A0.5 (0.5%)	88	102	86	29	58

Table 2. Chemical composition of raw (A and B) and purified (B0.5, B1, B2, B3, B4 and A0.5, A1, A2, A3, A4) bentonite samples

Chemical composition (% w/w)	LOI	SiO_2	Al_2O_3	Fe_2O_3	TiO_2	CaO	MgO	Na_2O	K_2O	Total
B (raw)	7.3	57.2	16.4	11.3	Traces	2.1	3.4	0.9	1.4	100.0
B4 (4%)	8.1	56.2	18.8	10.8	Traces	2.1	2.8	0.9	1.3	101.0
B3 (3%)	8.4	54.9	19.9	10.3	Traces	2.1	2.6	0.8	1.1	100.1
B2 (2%)	7.8	54.9	22.8	7.8	Traces	1.9	2.6	0.7	1.1	99.6
B1 (1%)	7.7	55.9	23.6	6.9	Traces	1.9	2.6	0.7	0.7	100.0
B0.5 (0.5%)	7.6	55.8	24.0	6.9	Traces	1.9	2.8	0.7	0.7	100.4
A (raw)	7.5	56.7	18.6	12.2	1.8	1.6	1.2	0.9	0.5	101.0
A4 (4%)	7.5	56.7	18.5	12.2	1.8	1.5	1.1	0.9	0.5	100.7
A3 (3%)	7.7	56.5	18.3	11.9	1.8	1.5	1.1	0.9	0.5	100.2
A2 (2%)	7.6	55.9	19.2	10.7	1.8	1.5	1.0	0.9	0.5	99.1
A1 (1%)	7.8	55.9	22.2	8.6	1.8	1.5	1.0	0.7	0.5	100.0
A0.5 (0.5%)	7.7	55.9	22.3	8.6	1.5	1.5	1.0	0.7	0.5	99.7

LOI, Loss on ignition measured at 850°C for 2 h.

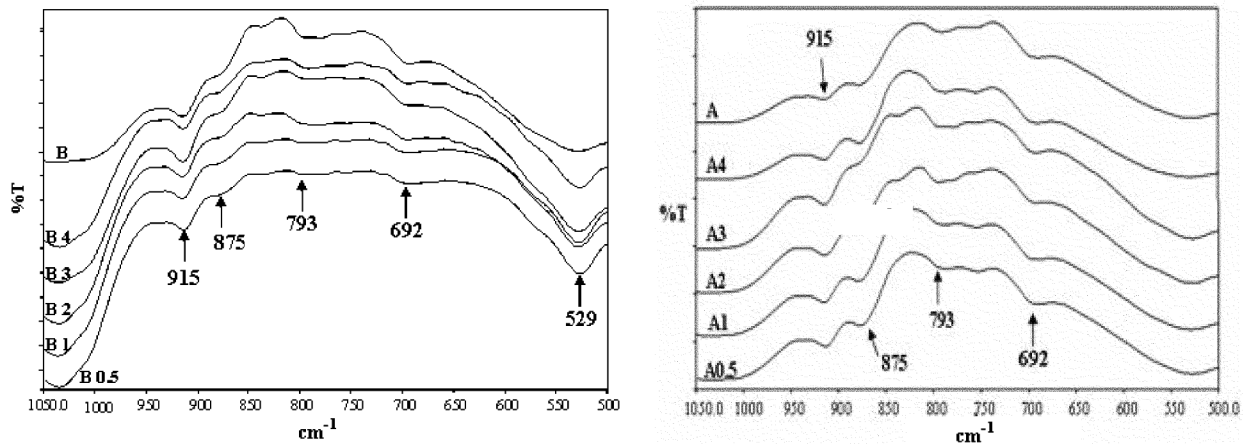

Figure 1. FT-IR spectrum of raw (A and B) and purified (B0.5, B1, B2, B3, B4 and A0.5, A1, A2, A3, A4) bentonite samples by sedimentation under different concentrations.

higher (60) compared to raw and purified bentonites at higher concentration (B, B4, B3 and B2). This is due to the removal of excessive iron-stained impurities which are responsible for the brownish-yellow colour of bentonite and is also evident from chemical composition as shown in Table 2.

Chemical analysis of raw and purified bentonite samples (Table 2) indicates the removal of excessive non-clay impurities at sedimentation carried out with lower viscosity and concentration. The amount of ferric oxide decreases up to about 7 wt% from 11.4 wt% (raw bentonite) with increase in alumina content from 16.4 to 24.0 wt% for samples B and B0.5 respectively. Quartz and calcite impurities are also removed during sedimentation up to 3% clay slurry, which also correlated with FT-IR and PXRD. Moisture content of all samples varies between 7 and 9 wt% and depends on the relative humidity during samples analysis. Loss on ignition which is carried out at 850°C in air atmosphere remains almost same for all samples.

FT-IR spectra of raw and purified bentonite samples recorded in the range 500–1050 cm^{-1} to study the effect of clay concentration during sedimentation technique are shown in Figure 1. IR peaks at 915, 875 and 793 cm^{-1} are attributed to AlAlOH, AlFeOH and platy form of tridymite bending vibration respectively[17,18]. The characteristic peak at 1115 cm^{-1} is due to Si–O stretching, out-of-plane Si–O stretching mode for montmorillonite. The band at 1035 cm^{-1} is attributed to Si–O stretching (in-plane) vibration for layered silicates. Intensity of vibrational peak at 915 (AlAlOH) and 529 cm^{-1} (Si–O bending) increases as the concentration of clay slurry decreases, which indicates an increase in montmorillonite content. Intensity of vibrational peak at 875 (AlFeOH) and 692 cm^{-1} (quartz) decreases and tends to diminish for lower clay concentration (B0.5 and B1), confirming the removal of iron-stained impurities and free silica from bentonite.

FT-IR spectra of purified bentonite (B0.5) and organoclays (CTA-clay and SMB-clay) are shown in Figure 2. The peaks between 3500 and 3700 cm^{-1} and near 3400 cm^{-1}

are indicative of montmorillonite-rich smectite clay. Peaks at 3620 and 3698 cm^{-1} are due to –OH band stretch for Al–OH and Si–OH. The shoulders and broadness of the –OH bands are mainly due to contributions of several structural –OH groups occurring in smectite. The overlaid absorption peaks in the region of 1640 cm^{-1} in the FT-IR spectrum of B0.5 is attributed to –OH bending mode of water (adsorbed water). IR peaks at 915, 875 and 836 cm^{-1} are attributed to AlAlOH, AlFeOH and AlMgOH bending vibration respectively. Peaks at 2940 and 2850 cm^{-1} for CTA-clay and SMB-clay respectively, are ascribed to the asymmetric and symmetric vibration of methylene groups $(CH_2)_n$ of the aliphatic carbon chain. In addition, there is also HCH stretching vibration band at 1465 cm^{-1} in the IR spectrum of both organoclays. FT-IR studies clearly indicate the formation of organic–inorganic hybrids.

The PXRD pattern (Figure 3 *a–c*) indicates the presence of impurities such as kaolin (K), quartz (Q) and calcite (Ca) in raw as well as purified bentonite samples, which are partly or to a great extent removed on further purification by sedimentation. Most of the quartz and calcite impurities are removed after sedimentation at 2 wt% clay slurry. There is no change in kaolin peak intensity, probably due to its fine particles and also less swelling ability of kaolinite mineral. Reflections relative to the planes [001], [003] and [130–200] confirmed the presence of montmorillonite with d_{001} ~ 1.2 nm for samples A and B, indicating the presence of sodium montmorillonite. It is clear from the PXRD pattern that sedimentation carried out by dispersing more than 2 wt% bentonite in deionized water is not able to remove non-clay impurities due to higher viscosity of the clay slurry. Therefore, it is preferred to suspend a lower amount of bentonite in deionized water for better beneficiation. PXRD study of B0.5, CTA-clay and SMB-clay was carried out within 2–10° (2θ), as shown in Figure 4. The d_{001} of purified bentonite and organoclay changes with respect to type of organic modifiers and varies with respect to alkyl chain length. The d_{001} of B0.5, CTA-clay and SMB-clay is 1.26 (2θ = 6.97), 1.92 (2θ = 4.61) and 2.56 nm (2θ = 3.45) respectively, which indicates that organic modifiers are intercalated into the interlayer spacing of bentonite.

Particle size distribution of purified bentonite (B0.5) was measured after the sample was dried and powdered. Particle size distribution, $d(0.5)$ of B0.5 dried, CTA-clay and SMB-clay is 8.7, 8.3 and 3.7 μm respectively. SMB-clay has finer particles with an average $d(0.5)$ = 3.7 μm compared to CTA-clay [$d(0.5)$ = 8.3 μm]. This could be

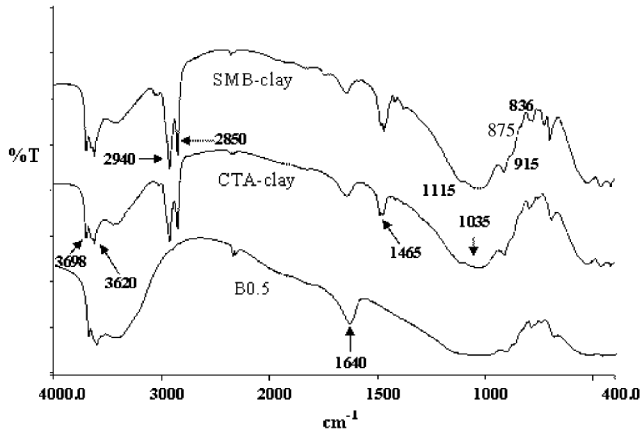

Figure 2. FT-IR spectrum of purified bentonite (B0.5) and organoclays (CTA-clay and SMB-clay).

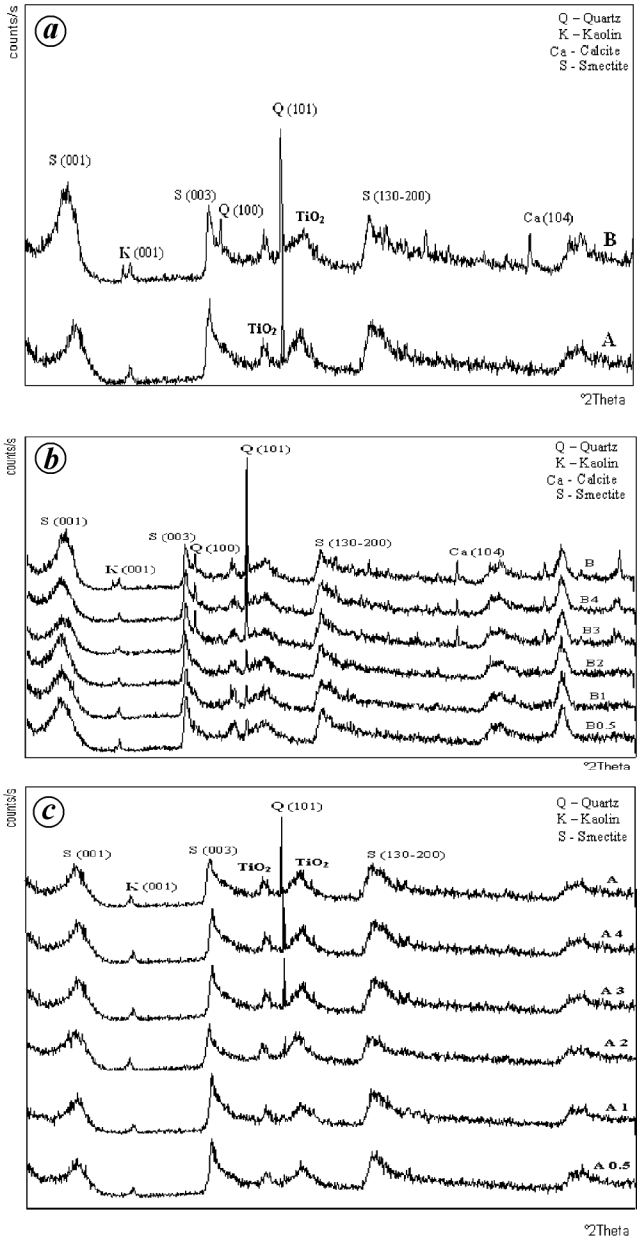

Figure 3. Powder X-ray diffraction patterns: ***a***, Raw bentonite, Cutch district (A) and Barmer district (B); ***b***, Raw bentonite (B) and purified bentonite (B0.5, B1, B2, B3 and B4), and ***c***, Raw bentonite (A) and purified bentonite (A0.5, A1, A2, A3 and A4).

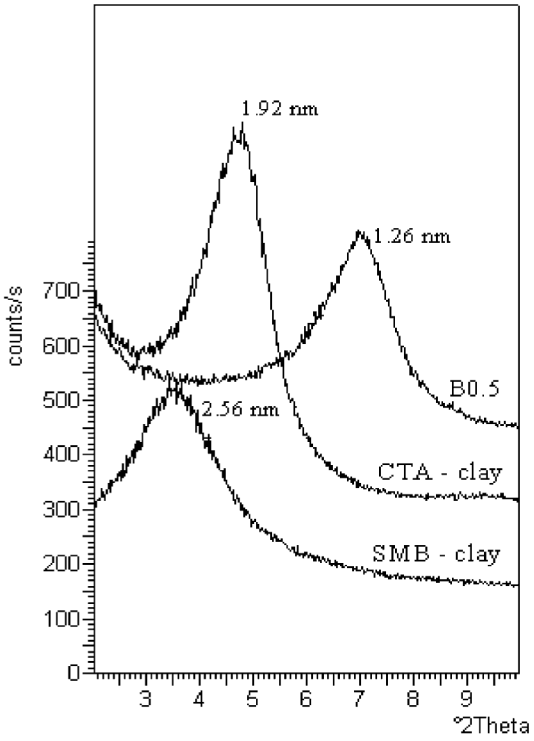

Figure 4. Powder X-ray diffraction pattern of B0.5, CTA-clay and SMB-clay.

attributed to longer alkyl chain or higher carbon atoms in SMB-clay compared to CTA-clay. Longer alkyl chains can cover silicate platelets more efficiently and does not allow agglomeration during drying compared to shorter alkyl chains.

Thermo-gravimetric analysis of B0.5, CTA-clay and SMB-clay was carried out within 50–850°C temperature range at the rate of 10°C/min in air atmosphere with a flow rate of 40 ml/min. Thermal stability of B0.5, CTA-clay and SMB-clay is shown in Figure 5; the peak decomposition temperature of B0.5, CTA-clay and SMB-clay is 450, 270 and 330°C respectively. B0.5 shows comparatively higher weight loss at <100°C than organoclays, which is due to loss of adsorbed water. Peak decomposition temperature for B0.5 at 450°C is due to loss of structural hydroxyl group. B0.5, CTA-clay and SMB-clay started to decompose at 180, 190 and 230°C. Thermal stability of SMB-clay is higher compared to CTA-clay because of the presence of an aromatic ring in the backbone chain of the strearyldimethylbenzylammonium cation.

Bentonite samples from Barmer district, Rajasthan and Cutch district, Gujarat were purified by sedimentation technique. Chemical composition, CEC, montmorillonite content, swelling indices and brightness indexes clearly indicate that most of the non-clay impurities such as quartz, iron-stained impurities and calcite can be removed from raw bentonite by suspending less than 2% bentonite in deionized water; this is also well-supported by FT-IR and

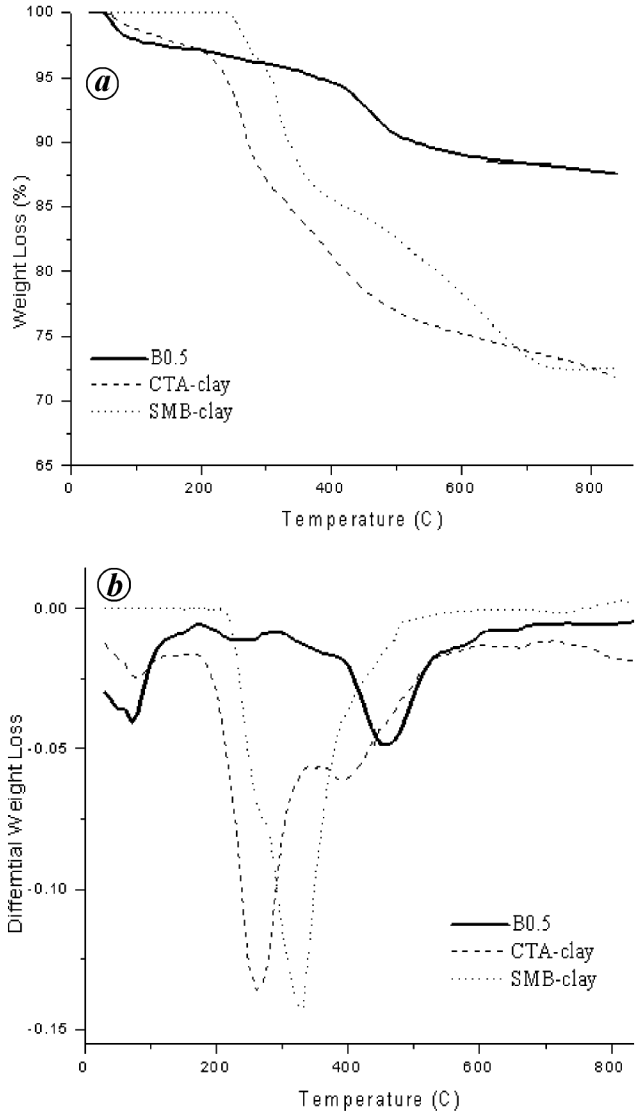

Figure 5. Thermo-gravimetric (*a*) and differential weight loss (*b*) of B0.5, CTA-clay and SMB-clay carried out up to 850°C at 10°C/min in air atmosphere with flow rate of 40 ml/min.

PXRD pattern. PXRD, FT-IR and CHN analysis confirm the formation of organic–inorganic hybrid. The d_{001} and particle size distribution of purified bentonite varies with the number of carbon atoms. Thermal stability of SMB-clay is higher due to the presence of an aromatic ring in the backbone of the organic modifier.

1. Grim, R. E. and Guven, N., *Bentonites – Geology, Mineralogy, Properties and Uses*, Elsevier Scientific, Amsterdam, 1978, pp. 229–232.
2. Theng, B. K. G., *The Chemistry of Clay-Organic Reactions*, John Wiley, New York, 1974.
3. Konta, J., Clay and man: Clay raw materials in the service of man. *Appl. Clay Sci.*, 1995, **10**, 275–335.

4. Ciullo, P. A., *White Bentonite – A Bright Future: An Industrial Minerals Special Review*, 1996, 2nd edn, pp. 18–22.
5. Lee, J. F., Mortland, M. M., Chiou, C. T., Kile, D. E. and Boyd, A., Adsorption of benzene, toluene and xylene by two tetramethylammonium-smectites having different charge densities. *Clays Clay Miner.*, 1990, **38**, 113–120.
6. Colin, C. H. and Murray, H. H., Industrial clays in the 21st century: A perspective of exploration, technology and utilization. *Appl. Clay Sci.*, 1997, **11**, 285–310.
7. Meier, L. P. and Kahr, G., Determination of cation exchange capacity of clay minerals using the complexes of copper (II) ion with triethylenetetramine and triethylenepentamine. *Clays Clay Miner.*, 1999, **47**, 386–388.
8. Patel, H. A., Somani, R. S., Bajaj, H. C. and Jasra, R. V., Nanoclays for polymer nanocomposites, paints, inks, greases and cosmetic formulations, drug delivery vehicle and wastewater treatment. *Bull. Mater. Sci.*, 2006, **29**, 133–145.
9. Thorson, T. A., Aerial surveying of Wyoming bentonite. *Appl. Clay Sci.*, 1997, **11**, 329–335.
10. Hassan, M. S. and Abdel-Khalek, N. A., Beneficiation and applications of an Egyptian bentonite. *Appl. Clay Sci.*, 1998, **13**, 99–115.
11. Plee, D., Gatineau, L. and Fripiat, J. J., Pillaring processes of smectites with and without tetrahedral substitution. *Clays Clay Miner.*, 1987, **35**, 81–88.
12. Colin, C. H. and Keeling, J., Categorization of industrial clays of Australia and New Zealand. *Appl. Clay Sci.*, 2002, **20**, 243–253.
13. Taylor, R. K., Cation exchange in clays and mud rocks. *J. Chem. Biotechnol. A*, 1985, **35**, 195–207.
14. Wilson, M. J., *A Handbook of Determination Methods in Clay Mineralogy*, Chapman and Hall, New York, 1987, pp. 26–131.
15. White, G. N., Berkheiser, V. E., Blanchard, F. N. and Hallmark, C. T., Thin-film analysis of clay particles using energy dispersive X-ray analysis. *Clays Clay Miner.*, 1982, **30**, 373–382.
16. Kaufhold, S., Dhimann, R., Ufer, K. and Meyer, F. M., Comparison of methods for the quantification of montmorillonite in bentonites. *Appl. Clay Sci.*, 2002, **22**, 145–151.
17. Tyagi, B., Chudasama, C. D. and Jasra, R. V., Determination of structural modification in acid activated montmorillonite clay by FT-IR spectroscopy. *Spectrochim. Acta, Part A*, 2006, **64**, 273–279.
18. Patel, H. A., Somani, R. S., Bajaj, H. C. and Jasra, R. V., Preparation and characterization of phosphonium montmorillonite with enhanced thermal stability. *Appl. Clay Sci.*, 2007, **35**, 194–200.

ACKNOWLEDGEMENTS. We thank Dr P. K. Ghosh, Director, Central Salt and Marine Chemicals Research Institute, Bhavnagar for interest in this work and also providing the facilities. We also thank CSIR, New Delhi for funding under a Network Project.

Received 31 July 2006; revised accepted 6 December 2006